



PAPER

Pauli-based fermionic teleportation with free massive particles by electron-exchange collisions

OPEN ACCESS

RECEIVED

26 September 2018

REVISED

24 January 2019

ACCEPTED FOR PUBLICATION

4 February 2019

PUBLISHED

28 March 2019

Original content from this work may be used under the terms of the [Creative Commons Attribution 3.0 licence](#).

Any further distribution of this work must maintain attribution to the author(s) and the title of the work, journal citation and DOI.

Bernd Lohmann^{1,2,3} and Karl Blum²¹ The Hamburg Centre For Ultrafast Imaging, Universität Hamburg, Luruper Chaussee 149, D-22761, Hamburg, Germany² Institut für Theoretische Physik, Westfälische Wilhelms-Universität Münster, Wilhelm-Klemm-Str. 9, D-48149, Münster, Germany³ Author to whom any correspondence should be addressed.E-mail: bernd.lohmann@desy.de and lohmanb@uni-muenster.de**Keywords:** non-locality, quantum teleportation, free massive particles, electron-exchange collision, Pauli-principle, entanglementSupplementary material for this article is available [online](#)

Abstract

Fundamental non-locality in quantum mechanical scattering processes is investigated by means of Fermionic teleportation. Our scenario employs free massive particles, electrons and atoms, within a twofold electron-exchange collision approach whereby, in the first collision, also generating the necessary spin–spin entanglement between initially unpolarized electrons and atoms. It is shown that in a second collision an arbitrary spin polarization state of a free electron can be teleported onto the other electron which has never been in contact with the first one. The underlying scheme relies on and is a direct consequence of the Pauli-principle and makes use of a high symmetry in spin space thereby avoiding restoration of the teleported states. The scattering process (teleportation) is highly symmetric allowing for interchanging the electronic and atomic constituents without loss of generality. Re-interpretation of Li and Na data reveals the feasibility and capability of Fermionic teleportation demonstrated by numerical and experimental data for the teleportation fidelity.

One of the most intriguing fundamentals of quantum mechanics is manifested in its non-locality. Criticized by Einstein *et al* [1] as ‘spooky action at a distance’ it has become an active and manifold area of research in recent years. A possible means in order to investigate such non-local phenomena has been provided by Bennett *et al* [2] in terms of quantum teleportation. It relies on the existence of long-range correlations between Einstein–Podolsky–Rosen (EPR) or Bell pairs and allows for a flawless transfer of quantum information between two constituents without contradicting the no-cloning theorem [3]. Since the pioneering experiment [4] applications in quantum communication and computing [5–9] have been pointed out illustrating the thriving research in this field. Astounding ‘ground-to-satellite quantum teleportation’ has just been reported [10]. All these approaches are either based on the direct use of photons or are mediated through light fields [11]. Beyond, it has been pointed out [12] that quantum mechanical methods and their alternatives can be tested for increasingly macroscopic systems [13] using the EPR paradox.

Taking up the idea, entanglement and EPR-based investigations must be recognized as being of considerable interest, particularly with massive particles. Caused by these demands, we enter new avenues and unveil a completely different scenario where, employing the methods of scattering theory, teleportation is emerging from a twofold elastic electron-exchange collision process with free, massive, Fermionic particles. As our approach deals with light atoms (Li, Na), coupling between spatial and spin variables is entirely due to the Pauli-principle, assisted by a high spin space symmetry, which is then responsible for the generation of correlations between the atomic and electronic spins. Advantageously, our scattering approach implicitly circumnavigates one of the drawbacks of photonic state-of-the-art quantum teleportation, i.e. its necessity to restore the quantum state by unitary transformation after teleportation [2].

As a prerequisite quantum teleportation relies on a suitably prepared entangled state which, in the photonic case, is provided via nonlinear parametric down conversion [14]. In our case, entanglement will be generated as a consequence of the Pauli-principle. In a first collision, unpolarized electrons and unpolarized atoms are

elastically scattered and their spins become entangled [15]. This entanglement can be found, and fixed in advance, by choosing appropriate scattering angles and/or energies. By varying the scattering parameters, the full range of spin–spin correlations can be generated, and in particular Bell-correlated spin pairs. Thus, the final spin system represents a tunable EPR resource [15, 16]. This is in contrast to realized entanglement generation between electrons as its creation is nonetheless photon-assisted [17]. Subsequently, a second electron with arbitrary (unknown) spin polarization is scattered from the atom and it is shown that its polarization state is non-locally teleported onto the first electron (still unpolarized after the first scattering). The experiment represents a single-outcome Bell measurement. Hence, restoration of the teleported state by unitary transformation [2], typical for the standard scheme, becomes obsolete in our approach.

The success of teleportation (fidelity) depends on the spin–spin correlations and again is directly related to the Pauli-principle. Re-interpretation of existing experimental and numerical sodium and lithium data [18–21], as well as recent calculations [22] underpins our results, revealing the feasibility and capability of such experiments. As an essential role is played by the Pauli-principle, we will refer to our approach as *Pauli-based Fermionic teleportation* (PBFT).

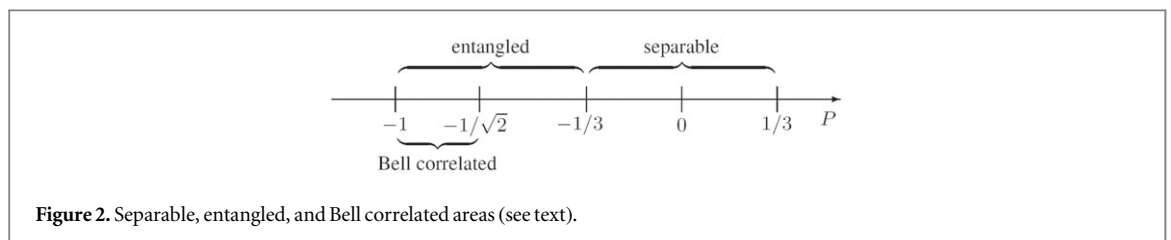
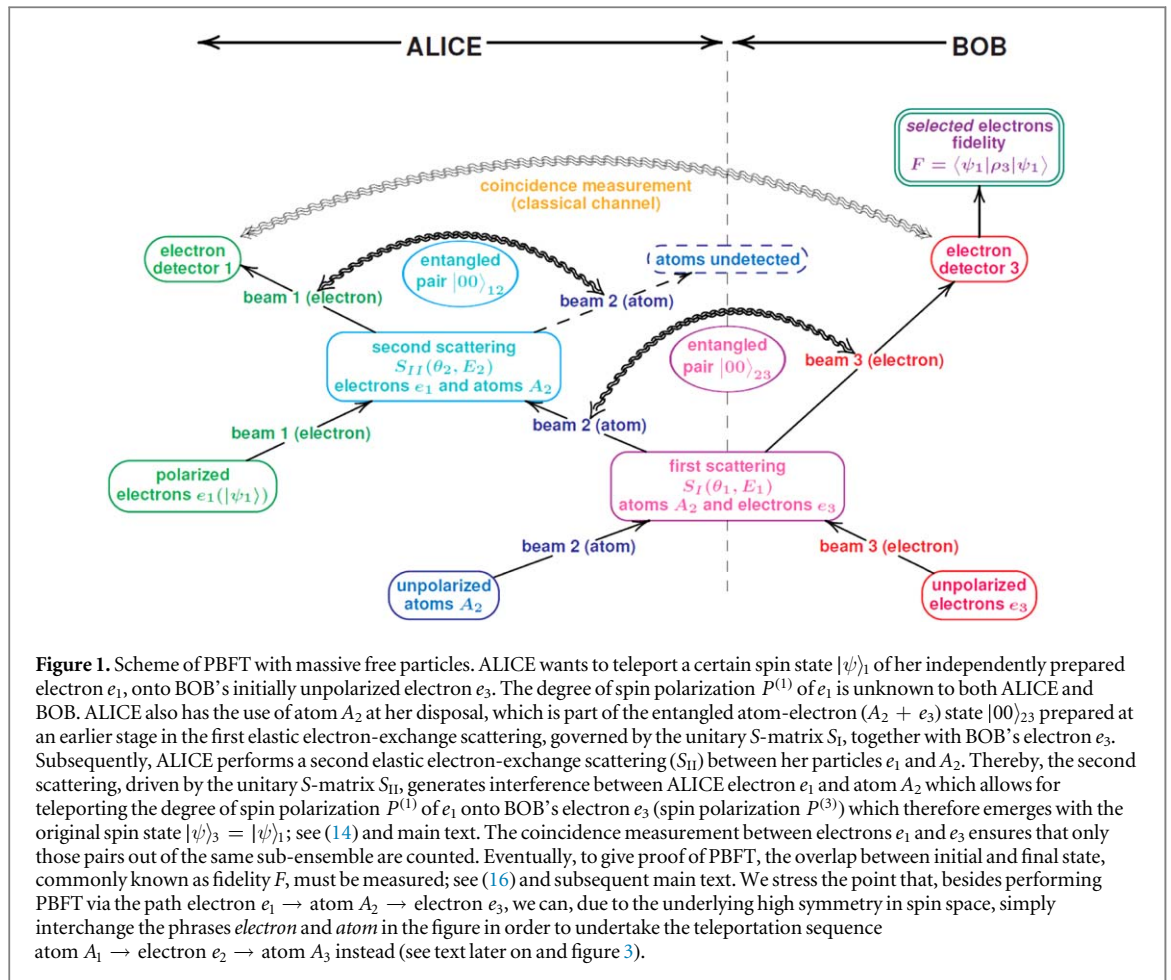
The paper is organized as follows. In the next section we will elucidate the underlying physics by considering a simple example first, assuming a maximally entangled EPR resource prepared in the first collision. The basic principles will be explained concentrating on pure states. In the following sections we will generalize the discussion. Firstly, we will consider the case where the electrons to be teleported are in a mixed state but still assuming the initially scattered particles to form the maximally entangled singlet state. Secondly, we will account for the general case in terms of density matrix where also the entangled particles can be in arbitrary states. In the last section we will introduce and adapt the concept of fidelity as a measure of success for teleportation and compare our predictions with pre-existing experimental sodium and lithium data. It will be shown that less-entangled mixed states can also be used as a resource for PBFT with fidelity beyond the boundary set by classical physics. For illustrative purposes, we will also provide videos of the numerical and experimental data. Finally, in the appendix we will present detailed derivations of the general formulas.

PBFT of a definite spin state

Quantum teleportation is a three-particle process where the quantum information of particle 1 is transferred onto particle 3 with the assistance of particle 2 in the absence of any direct quantum communication channels between them. In a first step two observers, ALICE and BOB, perform a specific elastic scattering process between quasi one-electron atoms (Na, Li) (particles 2) and electrons (particles 3), both initially unpolarized. Dealing with light atoms, all explicit spin-dependent interactions can be neglected in such an approach and, besides the Coulomb potential, electron-exchange is taken into account, only [23]. After the first scattering S_1 , with energy E_1 and scattering angle θ_1 (see figure 1), the final spin state of particles 2 and 3 is generally described by a spin-density matrix $\rho_{23} = T \rho_{\text{in}} T^\dagger$ where T denotes the transition operator and ρ_{in} describes the two-particle density matrix of the uncorrelated initial state. With the help of Clebsch–Gordan coefficients the T matrix elements can be coupled to their total spin S and magnetic component M_S which are both conserved during the collision. The T matrix does not depend on the magnetic components and hence, we are able to express the density matrix ρ_{23} in terms of scattering amplitudes $f^{(S)}$, ($S = 0, 1$). The spin-density matrix ρ_{23} can be completely characterized in terms of two individually measured polarization vectors, referring to particles 2 and 3, and the nine direct product components $\langle \sigma_i^{(2)} \times \sigma_j^{(3)} \rangle$ of the spin–spin correlation tensor ($i, j = x, y, z$). As shown in our previous research [15, 16], the polarization vectors of both particles remain zero under such conditions, as well as all non-diagonal components of the spin–spin correlation tensor, and the only non-vanishing parameters are the spin–spin correlation parameters

$$P_{23} = \langle \sigma_i^{(2)} \times \sigma_i^{(3)} \rangle = \frac{|f^{(1)}|^2 - |f^{(0)}|^2}{3 |f^{(1)}|^2 + |f^{(0)}|^2} \quad i = x, y, z, \quad (1)$$

where $f^{(1)}$ and $f^{(0)}$ denote the elastic triplet and singlet scattering amplitudes, respectively. Thus, the entanglement generating collision is characterized in terms of the single parameter $P_{23} = P_{23}(\theta_1, E_1)$ which is a function of scattering angle and energy. The correlation parameter can vary in the range $-1 \leq P_{23} \leq 1/3$. The spin–spin correlation parameter P_{23} is a direct measure of the entanglement properties of the final spin system [15, 16]. The spin system is separable if $|P_{23}| \leq 1/3$, and entangled in the region $-1 \leq P_{23} < -1/3$ (see figure 2). In particular, for $-1 \leq P_{23} \leq -1/\sqrt{2}$ the final spin states are Bell correlated, i.e. the CHSH-Bell inequality [24] is violated. Variation of scattering angle and/or energy changes the nature of the combined spin system from maximally entangled ($P_{23} = -1$) to completely chaotic ($P_{23} = 0$) and up to $P_{23} = 1/3$. It follows that the degree of entanglement is tunable and the desired value of P_{23} can be fixed in advance by choosing appropriate pairs of E_1 and θ_1 . It is of central importance that for a large variety of combinations (θ_1, E_1) the triplet amplitude $f^{(1)}$ vanishes and therefore the final spins form a pure singlet state corresponding to $P_{23} = -1$.



Required combinations of energy and angle can be read from the published data [15, 16, 22]. Choosing appropriate values of E_1 and θ_1 for ensuring $f^{(1)} = 0$ in the first scattering, the Pauli-principle requires particles 2 and 3 to be found in the maximally entangled singlet state

$$|00\rangle_{23} = \frac{1}{\sqrt{2}}(|\uparrow\rangle_2|\downarrow\rangle_3 - |\downarrow\rangle_2|\uparrow\rangle_3), \quad (2)$$

where $|\uparrow\rangle$ and $|\downarrow\rangle$ denote spin up and down, respectively, with respect to the laboratory z -axis. Equation (2) describes the spin part of the total wave function of the two–electron system after the first elastic collision S_I , where particles 2 refer to the bound valence shell s -electrons of the quasi one–electron atoms (Na, Li) while particles 3 describe a free electron beam in the sense of scattering theory; e.g. see [25]. As we are dealing with light atoms, spin–orbit coupling must not be accounted for. For a detailed proof and discussion we refer to the book by Kessler [23, particularly see ch 4]. Thus, one obtains information on the joint spin state of the pair but not on the individual spins. The described experiment must therefore be interpreted as a simple case of a Bell measurement. It is important to note that choosing spatial observables (θ_1, E_1) only, one can read off the spin–spin correlation parameter without performing a spin measurement. Since all explicitly spin–dependent interactions, and in particular spin–orbit coupling, can be neglected [15], the connection between the spatial and spin variables is entirely due to the Pauli-principle. Changing energy E_1 and/or scattering angle θ_1 changes the symmetry of the spatial wave function and the spin part must adapt accordingly leaving the total wave function antisymmetric. It is because of the central role of the Pauli-principle why we call the experiment described below as PBFT.

With the generated singlet state (2), PBFT can be performed (see figure 1). First, the entangled singlet pairs $|00\rangle_{23}$ are shared between ALICE and BOB (atoms to ALICE, electrons to BOB). ALICE has another source of electrons at her disposal (particles 1) prepared in a definite spin state

$$|\psi\rangle_1 = \alpha|\uparrow\rangle + \beta|\downarrow\rangle, \quad \text{with} \quad \alpha, \beta \in \mathbb{C}. \quad (3)$$

The normalization condition $|\alpha|^2 + |\beta|^2 = 1$ applies while the amplitudes are unknown to both ALICE and BOB. For instance, $|\psi\rangle_1$ has been independently prepared in another laboratory. It is most convenient, using the states $|\uparrow_a\rangle$ and $|\downarrow_a\rangle$ as basis instead of $|\uparrow\rangle$ and $|\downarrow\rangle$, and choose a as quantization axis such that the initial spin state of ALICE's electrons is represented by the state vector $|\psi\rangle_1 = |\uparrow_a\rangle$. The state $|\psi\rangle_1$ will be transferred to BOB via PBFT. This can be achieved performing a second elastic electron-exchange scattering of ALICE's electrons 1 from the atoms 2 in the same manner as discussed above. Applying an important property of the singlet state (2), its rotational symmetry in spin space, we can write down immediately its expression in the new basis (a -representation) as its representation remains invariant under rotations

$$|00\rangle_{23} = \frac{1}{\sqrt{2}}(|\uparrow_a\rangle_2|\downarrow_a\rangle_3 - |\downarrow_a\rangle_2|\uparrow_a\rangle_3). \quad (4)$$

Since ALICE's electrons 1 do not participate in the first collision S_I (see figure 1), the initial three-particle state before the second scattering S_{II} is given by the pure direct product state

$$|\psi_{\text{in}}\rangle = |\uparrow_a\rangle_1 \otimes |00\rangle_{23}, \quad (5)$$

which contains no correlations between the free electrons 1 and the entangled bound-free pair 2-3. Hence, substituting (4) into (5) yields the initial three-particle state $|\psi_{\text{in}}\rangle$ before the second collision as

$$|\psi_{\text{in}}\rangle = \frac{1}{\sqrt{2}}(|\uparrow_a\rangle_1|\uparrow_a\rangle_2|\downarrow_a\rangle_3 - |\uparrow_a\rangle_1|\downarrow_a\rangle_2|\uparrow_a\rangle_3). \quad (6)$$

We re-write the second term in (6) as the sum of the two Bell states $|00\rangle_{12}$ and $|10\rangle_{12} = \frac{1}{\sqrt{2}}(|\uparrow_a\rangle_1|\downarrow_a\rangle_2 + |\downarrow_a\rangle_1|\uparrow_a\rangle_2)$ and express $|\uparrow_a\rangle_1|\uparrow_a\rangle_2$ in the first term explicitly as the triplet state $|11\rangle_{12}$. Equation (6) can then be written in the form

$$|\psi_{\text{in}}\rangle = \frac{1}{\sqrt{2}} \left[|11\rangle_{12}|\downarrow_a\rangle_3 - \frac{1}{\sqrt{2}}(|10\rangle_{12} + |00\rangle_{12})|\uparrow_a\rangle_3 \right], \quad (7)$$

where $|11\rangle_{12}$ can also be expressed as the sum of two further Bell states.

Under the conditions stated above, the total spin S and component M_s are conserved during the second collision S_{II} and the scattering amplitudes are independent of M_s , which results in the simple transformation $|SM_s\rangle \rightarrow f^{(S)}|SM_s\rangle$. The crucial step is to choose E_2 and θ_2 such that the triplet amplitude $f^{(1)}(\theta_2, E_2)$ vanishes for this combination of scattering angle and energy. In this case we end up with the simple result

$$|\psi_{\text{in}}\rangle \xrightarrow{S_{II}} |\psi_{\text{out}}\rangle = -\frac{1}{2}f^{(0)}|00\rangle_{12} \otimes |\uparrow_a\rangle_3, \quad (8)$$

and after re-normalization

$$\begin{aligned} |\psi_{\text{out}}\rangle &= |00\rangle_{12} \otimes |\uparrow_a\rangle_3 \\ &= |00\rangle_{12} \otimes (\alpha|\uparrow\rangle_3 + \beta|\downarrow\rangle_3) = |00\rangle_{12} \otimes |\psi\rangle_3, \end{aligned} \quad (9)$$

where the last row in (9) has been rotated back and refer to the laboratory z -axis again. The definite quantum state (3) of ALICE has been teleported onto BOB's state, that is $|\psi\rangle_3 = |\psi\rangle_1$, and hence, PBFT succeeds. By choosing appropriate pairs of scattering angle and energy in order to ensure $f^{(1)}(\theta_2, E_2) = 0$ one can perfectly separate the $|00\rangle_{12}$ -part from all other Bell states in (7). Thus, the described process represents a single-outcome Bell measurement.

Initially, the electrons 1 have been in the definite (but unknown) state $|\psi\rangle_1$, independently prepared in another lab in advance. After the first scattering S_I , particles 2 and 3 were prepared maximally entangled in the singlet state and had no definite spin state of their own. After the second scattering S_{II} , particles 1 and 2 become maximally entangled. ALICE's electrons 1 have therefore completely lost their initial spin properties in accordance with the no-cloning theorem [3, 26] and, their initial state has been completely transferred to particles 3. BOB, receiving the classical information that ALICE obtained a count in her detector 1, while his detector 3 registers coincidentally, knows that his electron is in the state $|\psi\rangle_3$. The coincidence measurement between ALICE's electrons e_1 and BOB's e_3 ensures that only those pairs out of the same sub-ensemble are counted. A scheme of the full PBFT is shown in figure 1. As can be seen from (9), based on the Pauli-principle which overall governs the PBFT, and due to its high symmetry in spin space, no restoration of BOB's state $|\psi\rangle_3$ has become necessary. Particles 1 and 3 have never interacted directly during PBFT. It is important to note, that no spin measurement is and must be performed during PBFT. Any spin analysis at this stage disrupts the entanglement and PBFT cannot succeed. All that is known is that BOB's sub-ensemble of electrons, *selected* by

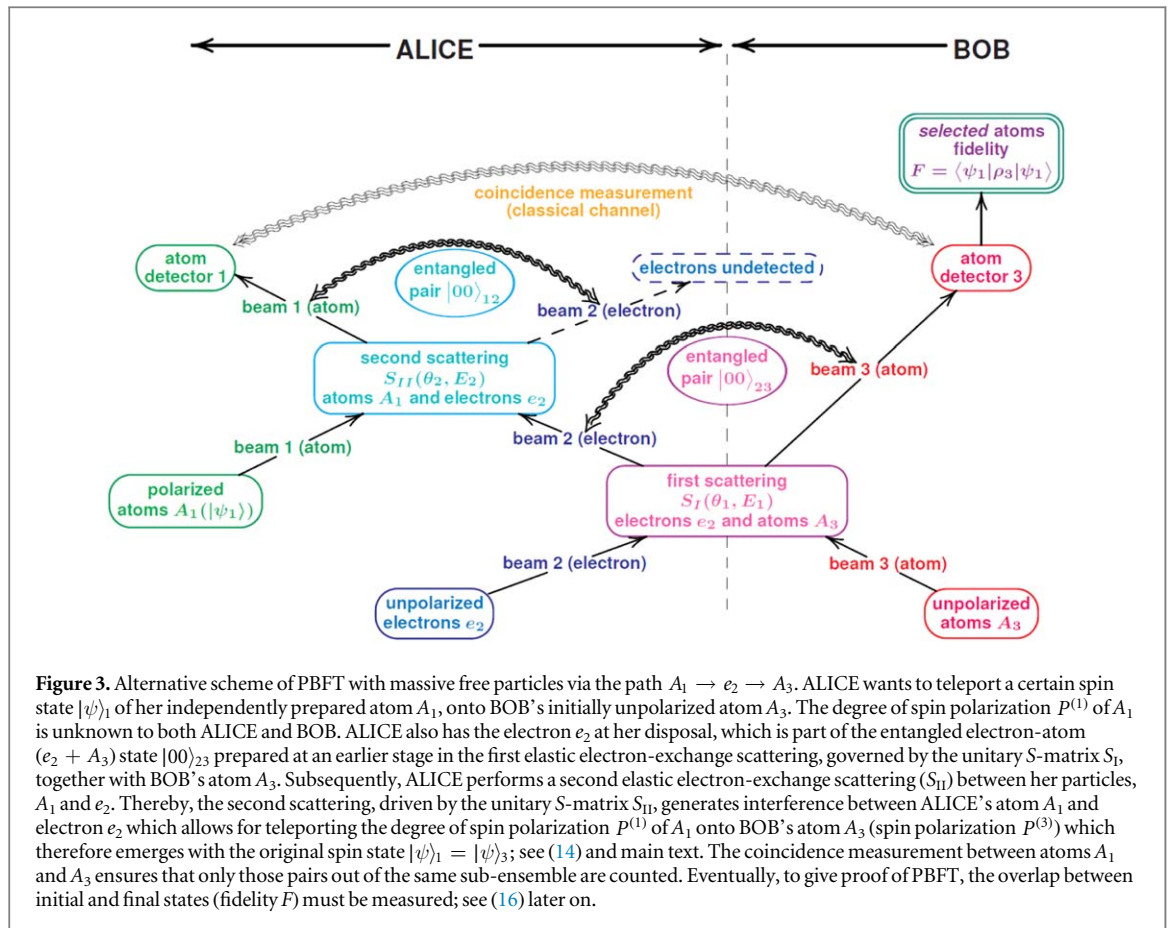


Figure 3. Alternative scheme of PBFT with massive free particles via the path $A_1 \rightarrow e_2 \rightarrow A_3$. ALICE wants to teleport a certain spin state $|\psi\rangle_1$ of her independently prepared atom A_1 , onto BOB's initially unpolarized atom A_3 . The degree of spin polarization $P^{(1)}$ of A_1 is unknown to both ALICE and BOB. ALICE also has the electron e_2 at her disposal, which is part of the entangled electron-atom ($e_2 + A_3$) state $|00\rangle_{23}$ prepared at an earlier stage in the first elastic electron-exchange scattering, governed by the unitary S -matrix S_I , together with BOB's atom A_3 . Subsequently, ALICE performs a second elastic electron-exchange scattering (S_{II}) between her particles, A_1 and e_2 . Thereby, the second scattering, driven by the unitary S -matrix S_{II} , generates interference between ALICE's atom A_1 and electron e_2 which allows for teleporting the degree of spin polarization $P^{(1)}$ of A_1 onto BOB's atom A_3 (spin polarization $P^{(3)}$) which therefore emerges with the original spin state $|\psi\rangle_1 = |\psi\rangle_3$; see (14) and main text. The coincidence measurement between atoms A_1 and A_3 ensures that only those pairs out of the same sub-ensemble are counted. Eventually, to give proof of PBFT, the overlap between initial and final states (fidelity F) must be measured; see (16) later on.

the coincidence measurement, is in the same states as particles 1. BOB could use his beam for further applications, e.g. as input in a second PBFT or other teleportation experiment. In addition, as a side effect, the initial entanglement has been completely transferred from the pair 2–3 to the pair 1–2. This is known as entanglement-swapping [27, 28]. In this respect the elastic electron-exchange collision can be considered as a unitary quantum gate.—Adapting the quantum marginal problem [29–31] to such a three-particle Fermionic system might yield a generalized scheme of PBFT. However, this query is beyond the scope of the present paper.—

Interchanging atoms and electrons

The discussed PBFT is highly symmetric. Particularly, the high symmetry in spin space enables us to simply interchange the words *electrons* and *atoms* in figure 1. Thereby, instead of teleporting the electron spin, we are able to teleport an unknown spin state of ALICE's atom A_1 onto BOB's atom A_3 employing the entanglement of ALICE's electron e_2 and a classical channel (coincidence measurement). For convenience, the atom $A_1 \rightarrow$ electron $e_2 \rightarrow$ atom A_3 PBFT is illustrated in figure 3. Both schemes have certain advantages in terms of fidelity measurement (spin analysis) or separation of the elastically scattered sub-ensembles of electrons or atoms after the first scattering process.

PBFT for mixed spin states

It is interesting that the derived results still hold if ALICE's electrons 1 are initially not in a definite but in an arbitrary spin state described by a density matrix ρ_1 . In diagonal form we have

$$\rho_1 = |\alpha|^2 |\uparrow_a\rangle_1 \langle \uparrow_a| + |\beta|^2 |\downarrow_a\rangle_1 \langle \downarrow_a|, \quad (10)$$

where $|\alpha|^2$ and $|\beta|^2$ are the respective probabilities. Since the overlap of the two terms in (10) is incoherent we can discuss them separately and add the results. As before, we assume particles 2 and 3 being in a singlet state, and scattering angle and energy in the second scattering, again, are chosen such that the triplet amplitude $f^{(1)}$ vanishes. Using (8) we obtain

$$\rho_{\text{in}} = \rho_1 \otimes |00\rangle_{23} \langle 00|_{23} \xrightarrow{S_{\text{II}}} \rho_{\text{out}} = |00\rangle_{12} \langle 00|_{12} \otimes \rho_3, \quad (11)$$

where the spin density matrix ρ_3 of BOB's *selected* electrons is given by the expression

$$\rho_3 = |\alpha|^2 |\uparrow_a\rangle_3 \langle \uparrow_a|_3 + |\beta|^2 |\downarrow_a\rangle_3 \langle \downarrow_a|_3. \quad (12)$$

As a result, PBFT is faithful independently of the initial state of ALICE's electrons, provided the triplet amplitude vanishes in both scattering processes.

PBFT for the general case

We will now consider the general case where the correlation parameters P_{12} and P_{23} of the first and second elastic scattering processes can have arbitrary values within their allowed range $[-1, 1/3]$. The derivation is straightforward but tedious (see appendix for calculational details) and the final expression for the reduced density matrix of BOB's *selected* particles 3 is given by

$$\rho_3 = \frac{1}{2} \begin{pmatrix} 1 + P_{12}P_{23} p_z^{(1)} & P_{12}P_{23}(p_x^{(1)} - ip_y^{(1)}) \\ P_{12}P_{23}(p_x^{(1)} + ip_y^{(1)}) & 1 - P_{12}P_{23} p_z^{(1)} \end{pmatrix}, \quad (13)$$

where $p_i^{(1)}$, ($i = x, y, z$) denotes the Cartesian components of the spin polarization vector of ALICE's initial electron beam. The spin polarization vectors of ALICE's beam 1 ($P^{(1)}$) and BOB's *selected* beam 3 ($P^{(3)}$) are therefore related by the simple expression (see appendix)

$$P^{(3)} = P_{12}P_{23}P^{(1)}. \quad (14)$$

This results in the (unknown) polarization vector $P^{(3)}$ being always parallel to $P^{(1)}$ for $P_{12}P_{23} > 0$ and anti-parallel for $P_{12}P_{23} < 0$. Comparing (9) and (14) it follows that the efficiency of the polarization teleportation is reduced by the factor $P_{12}P_{23}$.

Success of PBFT and fidelity

In order to get some idea of how faithful PBFT might be, we assume ALICE's original electron beam 1, which is to be teleported, as being in the definite (but unknown) state $|\uparrow_a\rangle$. In this case (13) reduces to (see appendix)

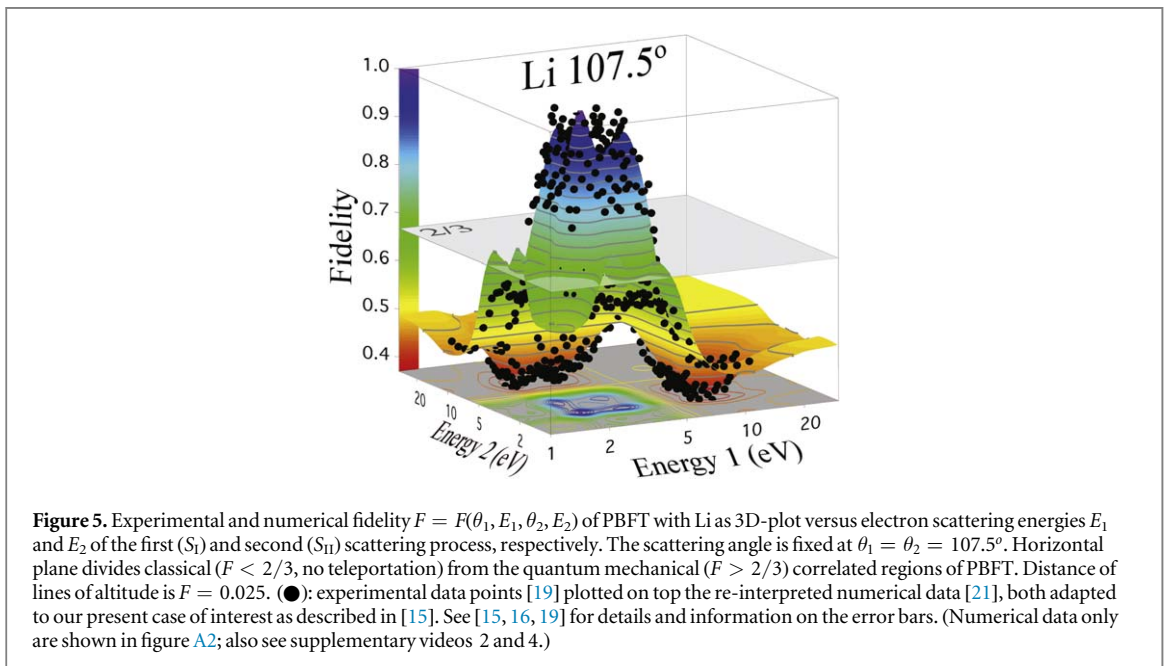
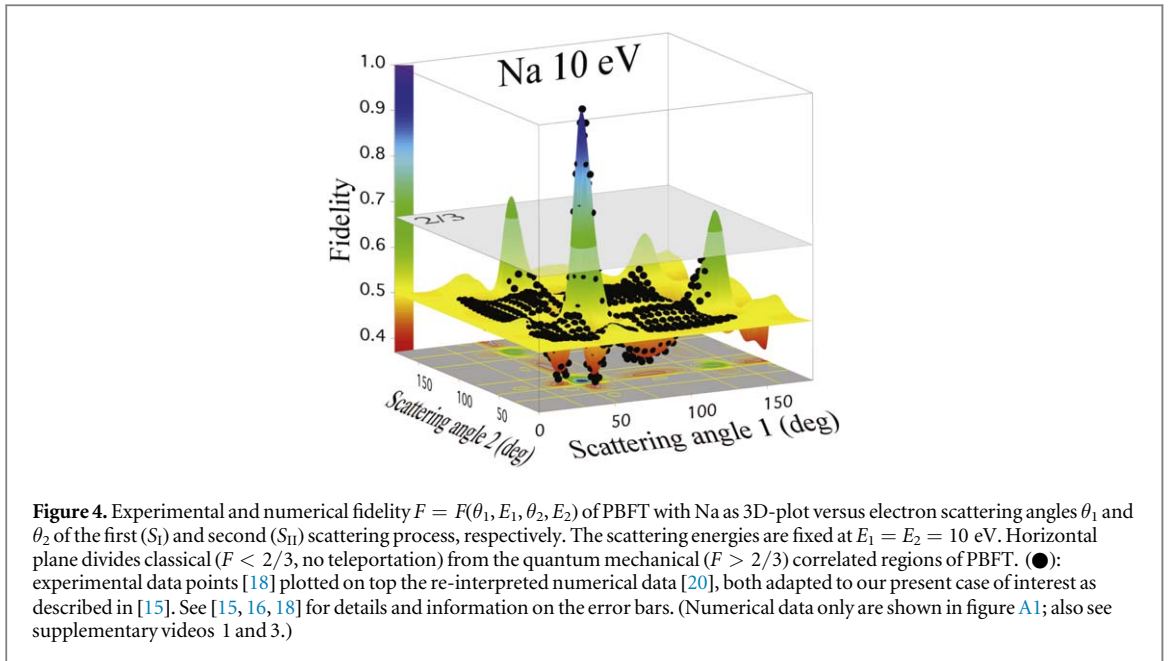
$$\rho_3 = \frac{1}{2} \begin{pmatrix} 1 + P_{12}P_{23} & 0 \\ 0 & 1 - P_{12}P_{23} \end{pmatrix}, \quad (15)$$

where we have again used the a -representation. The fidelity F , defined by the expression $F = \langle \uparrow_a | \rho_3 | \uparrow_a \rangle$, is a common and frequently used measure of success of quantum teleportation and hence, of PBFT. It yields the probability that a subset of BOB's *selected* electrons ρ_3 would pass a test for being in the state $|\psi_1\rangle$. From (15) we obtain

$$F = \frac{1}{2}(1 + P_{12}P_{23}). \quad (16)$$

For the general case with $|P^{(1)}| < 1$, we refer to (A.37) and the related section in the appendix. Hence, the fidelity F is directly related to the product $P_{12}P_{23}$ and is shown for Na in figure 4 as a 3D-plot versus the scattering angles θ_1 and θ_2 of the first and second scattering, respectively (also see supplementary video 1, available online at stacks.iop.org/NJP/21/033025/mmedia). The scattering energies are fixed in both collisions to $E_1 = E_2 = 10$ eV. Here, we used and re-interpreted existing experimental [18] and numerical [20] data (see figure A1 (in the appendix) and supplementary video 3 for the latter, only). The Li experimental [19] and numerical data [21] are presented in figure 5 in the same manner plotted versus the scattering energies E_1 and E_2 of the first and second scattering, respectively (also see supplementary video 2). The scattering angles of both collision processes have been fixed to $\theta_1 = \theta_2 = 107.5^\circ$ (see figure A2 (in the appendix) and supplementary video 4 for the numerical data, only). It is amazing that (13) and (14) apply to the full range of allowed values for the correlation parameter products, well outside the Bell region and even outside the entangled region; see figures 4 and 5 and figures A1 and A2 in the appendix (also see supplementary videos 1–4). Bennett *et al* [2] and Popescu [32] have already noted that teleportation could still be possible outside the Bell region but only with reduced efficiency. For the process considered here even separable mixtures can contribute but with even smaller efficiency.

If both scattering processes are pure singlet collisions, that is $P_{12} = P_{23} = -1$, we have $F = 1$ indicating a faithful teleportation from electrons 1 to electrons 3. This is achieved in both cases, Li and Na, at the maxima of the highest (blue) peaks; see figures 4 and 5 and supplementary videos 1 and 3. However, the overall structure of the two cases is different. In the sodium case there are single isolated peaks, only one of them showing large values of $P_{12}P_{23}$ and, hence, F up to one. For lithium there is a broad (blue-coloured) plateau with values of



$F > 0.9$ having peaks atop where $F = 1$ is clearly reached. F decreases steadily with decreasing values of P_{12} and P_{23} (also see the Li and Na supplementary videos).

Now, suppose that ALICE and BOB share no entangled state after the first scattering S_I but a separable mixture. Its density matrix ρ_{23} can always be written as a combination of direct product states. Physically, they are equivalent to mixtures, generated classically by ALICE and BOB agreeing, e.g. over the phone, on the local preparation of their respective states [16]. The electron pairs are still correlated but all correlations are of pure classical nature [15, 16] and therefore useless for quantum teleportation [32]. In the sodium case, this occurs for most of the angle combinations (θ_1, θ_2) of first and second scattering, respectively, as can be seen from the broad yellow coloured plane around $F \simeq 1/2$ displayed in figure 4 (also see figure A1 and supplementary videos 1 and 3).

The strongest correlation, obtainable for separable states, is $|P_{23}| = 1/3$, which yields fidelity $F = 2/3$, (with $P_{12} = -1$, and $P_{23} = -1/3$ in our scheme), shown as a horizontal plane in figures 4 and 5 (also in figures A1 and A2 and in the supplementary videos 1–4), representing the upper bound for classical transfer of information [32, 33]. In general, one says that any state is useful for teleportation if $F > 2/3$. In our scheme, this requires $P_{12}P_{23} > 1/3$. Assuming $P_{12} = -1$ it follows that any entangled state ρ_{23} , with $P_{23} < -1/3$, is useful for

teleportation in the sense of outperforming classical strategies; see figures 4 and 5 (also see figures A1 and A2, and supplementary videos 1–4). In particular, this result holds for states ρ_{23} with spin correlation parameters $-1/\sqrt{2} < P_{23} < -1/3$. Though entangled, these states do not violate the CHSH-Bell inequality [24]. Notwithstanding, they provide results $F > 2/3$ for the PBFT with fidelity up to $F = 0.854$ and hence, better than could ever be obtained by classical correlations and local operations.

Acknowledgments

The authors are grateful to Profs Drs M Drescher and G Alber, to PDs Drs A Dorn and R Moshhammer and to Drs B Langer and A Azima for helpful discussions and remarks during the preparation of the manuscript. We are most thankful to Dr B Langer for helpful assistance in the preparation of the figures and for preparing the videos. BL is thankful to Prof Dr M Drescher and The Hamburg Centre for Ultrafast Imaging (CUI) of the University of Hamburg for inviting him as Guest Scientist and for the hospitality extended to him during his stay. Generous financial support by the CUI which enabled for the finalization of the manuscript is gratefully acknowledged. The authors are thankful to Dr D Thompson for proof-reading the manuscript. We acknowledge support from the Open Access Publication Fund of the Westfälische Wilhelms-Universität Münster.

Appendix: Numerical fidelity of PBFT for Na and Li

For convenience we also included figures and supplementary videos of the numerical fidelity, only. For the sodium case in figure A1 (supplementary video 3) and for lithium in figure A2 (supplementary video 4), respectively.

PBFT for the general case

We will now consider the general case in detail where the spin–spin correlation parameters $P_{23} = P_{23}(\theta_1, E_1)$ and $P_{12} = P_{12}(\theta_2, E_2)$ of the first and second scattering can take on any value inside the allowed range $[-1, 1/3]$ depending on scattering angle and energy.

In the first collision unpolarized atoms and unpolarized electrons are scattered. As we have shown [15, 16], the final state after the first scattering is given by the density matrix

$$\begin{aligned} \rho_{23} = & \frac{1}{4} [(1 + P_{23}) |\uparrow\uparrow\rangle_{23} \langle\uparrow\uparrow|_{23} + (1 - P_{23}) |\uparrow\downarrow\rangle_{23} \langle\uparrow\downarrow|_{23} \\ & + 2P_{23} |\uparrow\downarrow\rangle_{23} \langle\downarrow\uparrow|_{23} + 2P_{23} |\downarrow\uparrow\rangle_{23} \langle\uparrow\downarrow|_{23} \\ & + (1 - P_{23}) |\downarrow\uparrow\rangle_{23} \langle\downarrow\uparrow| + (1 + P_{23}) |\downarrow\downarrow\rangle_{23} \langle\downarrow\downarrow|_{23}], \end{aligned} \quad (\text{A.1})$$

where particles 2 (ALICE's atom) and 3 (BOB's electron) are written in first and second position, respectively.

ALICE's electrons (particles 1) are assumed to be in a definite spin state

$$|\psi\rangle_1 = \alpha |\uparrow\rangle_1 + \beta |\downarrow\rangle_1, \quad \text{with } \alpha, \beta \in \mathbb{C}, \quad (\text{A.2})$$

with the normalization condition

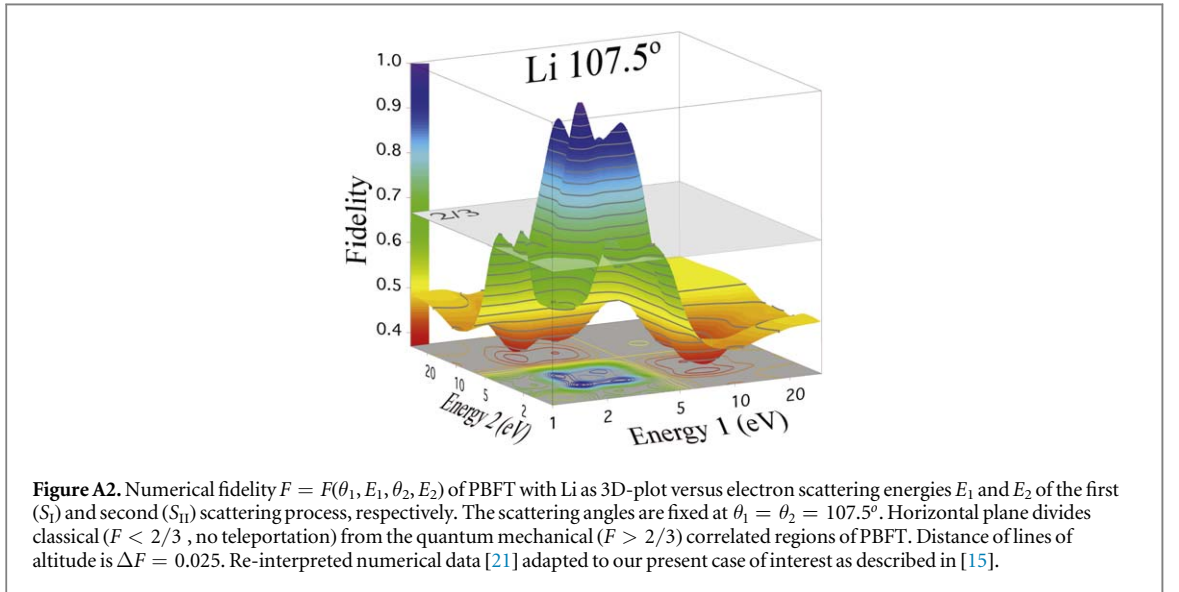
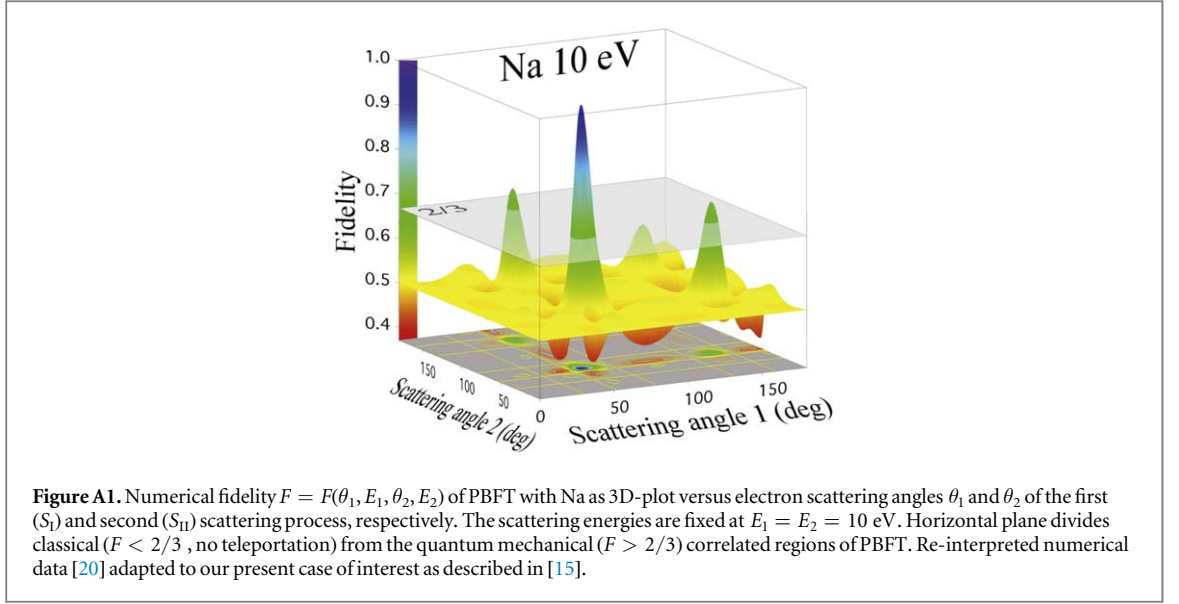
$$|\alpha|^2 + |\beta|^2 = 1, \quad (\text{A.3})$$

where the amplitudes are unknown to both, ALICE and BOB. Here, $|\uparrow\rangle$ and $|\downarrow\rangle$ describes states *spin up* and *spin down*, respectively, with respect to the laboratory z -axis which may even be unknown to ALICE. The state (A.2) describes a beam completely polarized with respect to a certain direction, say a . (That is, all electrons in $|\psi\rangle_1$ have *spin up* with respect to a .), and we can write

$$|\uparrow_a\rangle_1 = \alpha |\uparrow\rangle_1 + \beta |\downarrow\rangle_1. \quad (\text{A.4})$$

In the following, it is convenient to use a as quantization axis. It is essential in this respect that the matrix ρ_{23} remains invariant under rotations in spin space, that is, ρ_{23} keeps its form in any rectangular system, the laboratory system x, y, z as in (A.1) or in the a -system with axes a, a', a'' . Therefore, we can write the initial three-particle system in the a -representation, simply by substituting $|\uparrow\rangle \rightarrow |\uparrow_a\rangle$ and $|\downarrow\rangle \rightarrow |\downarrow_a\rangle$ in ρ_{23} for particles 2 and 3, respectively. Thus, we explicitly write the initial three particle state before the second scattering as

$$\begin{aligned} \rho_{in} = & \frac{1}{4} \{ |\uparrow_a \uparrow_a\rangle_{12} \langle\uparrow_a \uparrow_a|_{12} \otimes [(1 + P) |\uparrow_a\rangle_3 \langle\uparrow_a|_3 + (1 - P) |\downarrow_a\rangle_3 \langle\downarrow_a|_3] \\ & + |\uparrow_a \downarrow_a\rangle_{12} \langle\uparrow_a \downarrow_a|_{12} \otimes [(1 - P) |\uparrow_a\rangle_3 \langle\uparrow_a|_3 + (1 + P) |\downarrow_a\rangle_3 \langle\downarrow_a|_3] \\ & + |\uparrow_a \uparrow_a\rangle_{12} \langle\uparrow_a \downarrow_a|_{12} \otimes 2P |\downarrow_a\rangle_3 \langle\uparrow_a|_3 + |\uparrow_a \downarrow_a\rangle_{12} \langle\uparrow_a \uparrow_a|_{12} \otimes 2P |\uparrow_a\rangle_3 \langle\downarrow_a|_3 \}, \end{aligned} \quad (\text{A.5})$$



where \otimes denotes the direct product. Here and in the following, we abbreviate the correlation parameter of the first scattering as $P = P_{23}$ if not causing ambiguities.

We will now consider the electron-exchange scattering between ALICE's electrons (particles 1) and the quasi one-electron atoms (particles 2) described by the scattering matrix S_{II} . The total spin S and its component M_s in the direction of the quantization axis a remain constant, and the scattering amplitudes are independent of M_s . The collision between particles in the states $|\uparrow_a\rangle_1|\uparrow_a\rangle_2$ and $|\downarrow_a\rangle_1|\downarrow_a\rangle_2$ are therefore pure triplet transitions,

$$|\uparrow_a\uparrow_a\rangle_{12} \xrightarrow{S_{II}} f^{(1)} |\uparrow_a\uparrow_a\rangle_{12}, \quad (\text{A.6a})$$

and

$$|\downarrow_a\downarrow_a\rangle_{12} \xrightarrow{S_{II}} f^{(1)} |\downarrow_a\downarrow_a\rangle_{12}. \quad (\text{A.6b})$$

In contrast, the states $|\uparrow_a\rangle_1|\downarrow_a\rangle_2$ and $|\downarrow_a\rangle_1|\uparrow_a\rangle_2$ can be written as a combination of the triplet $|10\rangle_{12}$ and singlet state $|00\rangle_{12}$, respectively,

$$|\uparrow_a\downarrow_a\rangle_{12} = \frac{1}{\sqrt{2}}(|10\rangle_{12} + |00\rangle_{12}), \quad (\text{A.6c})$$

and

$$|\downarrow_a\uparrow_a\rangle_{12} = \frac{1}{\sqrt{2}}(|10\rangle_{12} - |00\rangle_{12}). \quad (\text{A.6d})$$

Thus, we have the transitions

$$|\uparrow_a \downarrow_a\rangle_{12} \xrightarrow{S_{II}} \frac{1}{\sqrt{2}}(f^{(1)} |10\rangle_{12} + f^{(0)} |00\rangle_{12}), \quad (\text{A.6e})$$

and

$$|\downarrow_a \uparrow_a\rangle_{12} \xrightarrow{S_{II}} \frac{1}{\sqrt{2}}(f^{(1)} |10\rangle_{12} - f^{(0)} |00\rangle_{12}). \quad (\text{A.6f})$$

Equivalently, we introduce direct and exchange amplitudes [23], f and g , writing the following possibilities with respect to the contributing electronic spins

$$|\uparrow_a\rangle_1 |\downarrow_a\rangle_2 \xrightarrow{S_{II}} f |\uparrow_a\rangle_1 |\downarrow_a\rangle_2 - g |\downarrow_a\rangle_1 |\uparrow_a\rangle_2, \quad (\text{A.7a})$$

$$|\downarrow_a\rangle_1 |\uparrow_a\rangle_2 \xrightarrow{S_{II}} f |\downarrow_a\rangle_1 |\uparrow_a\rangle_2 - g |\uparrow_a\rangle_1 |\downarrow_a\rangle_2, \quad (\text{A.7b})$$

$$|\uparrow_a\rangle_1 |\uparrow_a\rangle_2 \xrightarrow{S_{II}} (f - g) |\uparrow_a\rangle_1 |\uparrow_a\rangle_2, \quad (\text{A.7c})$$

$$|\downarrow_a\rangle_1 |\downarrow_a\rangle_2 \xrightarrow{S_{II}} (f - g) |\downarrow_a\rangle_1 |\downarrow_a\rangle_2. \quad (\text{A.7d})$$

The term $(f - g)$ is known as the interference amplitude. Note, that the minus sign is implicitly taking care of the Pauli-principle. The amplitudes f and g are related to the triplet and singlet scattering amplitudes $f^{(1)}$ and $f^{(0)}$ by the relations, e.g. [23, 34, 35],

$$f = \frac{1}{2}(f^{(1)} + f^{(0)}), \quad \text{and} \quad g = \frac{1}{2}(f^{(0)} - f^{(1)}), \quad (\text{A.8a})$$

and the inverse relations

$$f^{(1)} = f - g, \quad \text{and} \quad f^{(0)} = f + g. \quad (\text{A.8b})$$

From (A.8) we obtain the useful relations

$$|f|^2 + |g|^2 = \frac{1}{2}(|f^{(1)}|^2 + |f^{(0)}|^2), \quad (\text{A.9a})$$

and

$$fg^* + f^*g = \frac{1}{2}(|f^{(0)}|^2 - |f^{(1)}|^2). \quad (\text{A.9b})$$

Substituting the appropriate relations (6) and (7) into (A.5) and, with the help of relations (8), expressing all interference amplitudes $(f - g)$ in terms of triplet amplitudes, we obtain after some rearrangements the (un-normalized) final state density matrix after the second collision as

$$\begin{aligned} \rho_{out} = & \frac{1}{4} \{ (|f^{(1)}|^2 |\uparrow_a \uparrow_a\rangle_{12} \langle \uparrow_a \uparrow_a|_{12}) \otimes [(1 + P) |\uparrow_a\rangle_3 \langle \uparrow_a|_3 + (1 - P) |\downarrow_a\rangle_3 \langle \downarrow_a|_3] \\ & + (|f|^2 |\uparrow_a \downarrow_a\rangle_{12} \langle \uparrow_a \downarrow_a|_{12} + |g|^2 |\downarrow_a \uparrow_a\rangle_{12} \langle \downarrow_a \uparrow_a|_{12}) \\ & \otimes [(1 - P) |\uparrow_a\rangle_3 \langle \uparrow_a|_3 + (1 + P) |\downarrow_a\rangle_3 \langle \downarrow_a|_3] \\ & - (fg^* |\uparrow_a \downarrow_a\rangle_{12} \langle \downarrow_a \uparrow_a|_{12} + f^*g |\downarrow_a \uparrow_a\rangle_{12} \langle \uparrow_a \downarrow_a|_{12}) \\ & \otimes [(1 - P) |\uparrow_a\rangle_3 \langle \uparrow_a|_3 + (1 + P) |\downarrow_a\rangle_3 \langle \downarrow_a|_3] \\ & + (f^{(1)} f^* |\uparrow_a \uparrow_a\rangle_{12} \langle \uparrow_a \downarrow_a|_{12} - f^{(1)} g^* |\uparrow_a \uparrow_a\rangle_{12} \langle \downarrow_a \uparrow_a|_{12}) \otimes 2P |\downarrow_a\rangle_3 \langle \uparrow_a|_3 \\ & + (f^{(1)*} f |\uparrow_a \downarrow_a\rangle_{12} \langle \uparrow_a \uparrow_a|_{12} - f^{(1)*} g |\uparrow_a \downarrow_a\rangle_{12} \langle \uparrow_a \uparrow_a|_{12}) \otimes 2P |\uparrow_a\rangle_3 \langle \downarrow_a|_3 \}. \end{aligned} \quad (\text{A.10})$$

Normalization and differential cross section

Building the trace, we sum over the diagonal elements of (A.10) which results in

$$\begin{aligned} \text{Tr } \rho_{out} &= \frac{1}{4} \{ |f^{(1)}|^2 [(1 + P) + (1 - P)] + (|f|^2 + |g|^2) [(1 - P) + (1 + P)] \} \\ &= \frac{1}{2} (|f^{(1)}|^2 + |f|^2 + |g|^2). \end{aligned} \quad (\text{A.11})$$

Applying the identity (9), we remain with

$$\text{Tr } \rho_{out} = \frac{1}{4} (3 |f^{(1)}|^2 + |f^{(0)}|^2) = \sigma_{12}, \quad (\text{A.12})$$

where we introduce the differential cross section σ_{12} of the second scattering process performed by ALICE alone. Thus, we write the normalized density matrix as

$$\rho_{\text{out}}^{(n)} = \frac{1}{\sigma_{12}} \rho_{\text{out}}. \quad (\text{A.13})$$

BOB's reduced density matrix

In order to compare the final state of BOB's electron (after having selected the relevant sub-ensemble by performing the coincidence experiment), we calculate the 2×2 reduced density matrix ρ_3 , defined by the expression, see [36],

$$\rho_3 = \text{Tr}_{1,2} \rho_{\text{out}}^{(n)} = \sum_{M_1, M_2} \langle M_1 M_2 | \rho_{\text{out}} | M_1 M_2 \rangle. \quad (\text{A.14})$$

Thus, we have to sum over the elements of (A.10), diagonal in M_1 and M_2 (particles 1 and 2 owned by ALICE) and obtain the normalized reduced density matrix

$$\begin{aligned} \rho_3^{(n)} = \frac{1}{4\sigma_{12}} \{ & |f^{(1)}|^2 [(1+P)|\uparrow_a\rangle_3 \langle\uparrow_a|_3 + (1-P)|\downarrow_a\rangle_3 \langle\downarrow_a|_3] \\ & + (|f|^2 + |g|^2) [(1-P)|\uparrow_a\rangle_3 \langle\uparrow_a|_3 + (1+P)|\downarrow_a\rangle_3 \langle\downarrow_a|_3] \}. \end{aligned} \quad (\text{A.15})$$

Expressing the direct and exchange amplitudes in terms of the singlet and triplet ones by using (A.9) and applying (A.12), we obtain

$$\begin{aligned} \rho_3^{(n)} = \frac{1}{8\sigma_{12}} \{ & 2 |f^{(1)}|^2 [(1+P)|\uparrow_a\rangle_3 \langle\uparrow_a|_3 + (1-P)|\downarrow_a\rangle_3 \langle\downarrow_a|_3] \\ & + (|f^{(1)}|^2 + |f^{(0)}|^2) [(1-P)|\uparrow_a\rangle_3 \langle\uparrow_a|_3 + (1+P)|\downarrow_a\rangle_3 \langle\downarrow_a|_3] \}. \end{aligned} \quad (\text{A.16})$$

As can be seen from (A.16) the density matrix $\rho_3^{(n)}$ is diagonal with respect to particle 3 (BOB's electron). This is due to our chosen coordinate frame within the a -representation.

Calculating the matrix elements $\langle M_3 | \rho_3^{(n)} | M_3 \rangle$ and explicitly re-expressing the correlation parameter $P = P_{23}$ yields

$$\begin{aligned} \langle \uparrow_a | \rho_3^{(n)} | \uparrow_a \rangle &= \frac{1}{8\sigma_{12}} [3 |f^{(1)}|^2 + |f^{(0)}|^2 + P_{23} (|f^{(1)}|^2 - |f^{(0)}|^2)] \\ &= \frac{1}{2} \left(1 + P_{23} \frac{|f^{(1)}|^2 - |f^{(0)}|^2}{4\sigma_{12}} \right), \end{aligned} \quad (\text{A.17})$$

where we used (A.12) for the differential cross section σ_{12} of the second scattering process. In full analogy to the first collision process S_I , we introduce the correlation parameter

$$P_{12} = \frac{|f^{(1)}|^2 - |f^{(0)}|^2}{3 |f^{(1)}|^2 + |f^{(0)}|^2}, \quad (\text{A.18})$$

which drives the second electron exchange-scattering S_{II} . Thus, we end up with the diagonal matrix elements

$$\langle \uparrow_a | \rho_3^{(n)} | \uparrow_a \rangle = \frac{1}{2} (1 + P_{12} P_{23}), \quad (\text{A.19a})$$

and due to symmetry requirements

$$\langle \downarrow_a | \rho_3^{(n)} | \downarrow_a \rangle = \frac{1}{2} (1 - P_{12} P_{23}). \quad (\text{A.19b})$$

In explicit matrix form we write

$$\rho_3 = \frac{1}{2} \begin{pmatrix} 1 + P_{12} P_{23} & 0 \\ 0 & 1 - P_{12} P_{23} \end{pmatrix}, \quad (\text{A.20})$$

which refers to (15) in the main text. Here and in the following we suppress the upper index (n) if not causing ambiguities. The matrix element (19) gives the possibility of finding an electron in state $|\uparrow_a\rangle_3$ if a measurement is performed. This matrix element, commonly called fidelity F , is often used as a measure of success for the teleportation process [32]. If ALICE and BOB share a singlet state ($P_{23} = -1$), and if the second collision is again pure singlet scattering ($P_{12} = -1$), we obtain from (A.20)

$$\rho_3 = |\uparrow_a\rangle_3 \langle\uparrow_a|_3, \quad (\text{A.21})$$

indicating a faithful quantum teleportation. It should be noted that F captures only the mean value behaviour of BOB's output state. The use of the fidelity for characterizing quantum teleportation is therefore limited.

Let us now analyse whether other states besides the maximally entangled singlets can be used for quantum teleportation. Any state with $|P_{23}| \leq 1/3$ is separable and can be written as a direct product of particles 2 and 3. It can be prepared by ALICE and BOB in a classical way, that is, by agreeing over phone on the local preparation

of their respective states. Hence, the spin correlations are classical, that is they can be considered as prearranged by ALICE and BOB [15, 16].

Any direct product (entangled) state is useless for teleportation as for such states manipulation of particle 2 during the second scattering has no effect on what can be predicted on particle 3. Whereas particles 1 and 2 become entangled, particles 3 are unaffected and keep their state obtained during the first collision. One can still find a certain number of BOB's particles in state $|\uparrow_a\rangle_3$ but this is a classical effect based on classical statistics. The best result for these *classical* mixtures is obtained for $P_{23} = -1/3$ and $P_{12} = -1$ giving fidelity $F = 2/3$ [32].

Finally, let us consider the spin polarization. Since ρ_3 is diagonal in the a -representation, the spin polarization vector $P^{(3)}$ of BOB's selected electrons is directed along a . Its magnitude is given by the difference of the two diagonal elements of (A.20), that is

$$|P^{(3)}| = P_{12}P_{23}. \quad (\text{A.22})$$

Since the spin polarization vector of ALICE's initial electron beam is also oriented along a , we can write in vector notation

$$P^{(3)} = P_{12}P_{23}P^{(1)}, \quad (\text{A.23})$$

which gives (14) in the main text.

The spin polarization vector is necessarily parallel or anti-parallel to $P^{(1)}$ depending on the sign of the product $P_{12}P_{23}$. For $P_{12}P_{23} = 1$, we have $P^{(3)} = P^{(1)}$ indicating a faithful quantum teleportation. $P_{12}P_{23}$ can also be used as a measure of success.

We will now transform back to the xyz -coordinate frame (laboratory frame). Using (A.4)

$$|\psi\rangle_1 = |\uparrow_a\rangle = \alpha |\uparrow\rangle_1 + \beta |\downarrow\rangle_1, \quad (\text{A.24a})$$

and

$$|\downarrow_a\rangle = \beta^* |\uparrow\rangle_1 - \alpha^* |\downarrow\rangle_1, \quad (\text{A.24b})$$

where $|\uparrow_a\rangle$ and $|\downarrow_a\rangle$ denote the spin states with respect to direction a , we write BOB's density matrix in the form

$$\rho_3 = \frac{1}{2}[(1 + P_{12}P_{23})|\uparrow_a\rangle\langle\uparrow_a| + (1 - P_{12}P_{23})|\downarrow_a\rangle\langle\downarrow_a|]. \quad (\text{A.25})$$

Substituting the relations (24) into (A.25) and expressing the results in explicit matrix form, we obtain BOB's density matrix ρ_3 in the xyz -system

$$\rho_3 = \frac{1}{2} \begin{pmatrix} 1 + P_{12}P_{23}(|\alpha|^2 - |\beta|^2) & 2P_{12}P_{23} 2\alpha\beta^* \\ 2P_{12}P_{23} 2\alpha^*\beta & 1 - P_{12}P_{23}(|\alpha|^2 - |\beta|^2) \end{pmatrix}. \quad (\text{A.26})$$

The amplitudes α and β in (A.26) are related to the components of the spin polarization vector $P^{(1)}$ of ALICE's electrons, defined by the relation

$$\langle\psi_1|\sigma_i|\psi_1\rangle = p_i^{(1)}, \quad i = x, y, z, \quad (\text{A.27})$$

where σ_i denote the relevant Pauli matrices. We obtain

$$p_x^{(1)} = \alpha\beta^* + \alpha^*\beta, \quad (\text{A.28a})$$

$$p_y^{(1)} = i(\alpha\beta^* - \alpha^*\beta), \quad (\text{A.28b})$$

and

$$p_z^{(1)} = |\alpha|^2 - |\beta|^2. \quad (\text{A.28c})$$

Inserting (28) into (A.26) and parametrizing the density matrix ρ_3 in terms of the spin polarization vector components $p_i^{(3)}$, ($i = x, y, z$) of BOB's sub-ensemble of electrons, selected in the coincidence experiment, we obtain after some rearrangements

$$\begin{aligned} \rho_3 &= \frac{1}{2} \begin{pmatrix} 1 + p_z^{(3)} & p_x^{(3)} - ip_y^{(3)} \\ p_x^{(3)} - ip_y^{(3)} & 1 - p_z^{(3)} \end{pmatrix} \\ &= \frac{1}{2} \begin{pmatrix} 1 + P_{12}P_{23} p_z^{(1)} & 2P_{12}P_{23}(p_x^{(1)} - ip_y^{(1)}) \\ 2P_{12}P_{23}(p_x^{(1)} - ip_y^{(1)}) & 1 - P_{12}P_{23} p_z^{(1)} \end{pmatrix}. \end{aligned} \quad (\text{A.29})$$

Eventually, we derive expressions for the spin polarization vector $P^{(3)}$ of BOB's sub-ensemble of electrons *selected* by the coincidence measurement; see figure 1. Using the relation

$$p_i^{(3)} = \text{Tr } \rho_3 \sigma_i, \quad (\text{A.30})$$

we obtain the general expression

$$P^{(3)} = P_{12} P_{23} P^{(1)}. \quad (\text{A.31})$$

The result (A.31) shows that the spin polarization vectors of particles 3 (BOB's electrons) and that of particles 1 (ALICE's electrons) are always parallel or anti-parallel depending on the sign of $P_{12}P_{23}$. In the case where the scattering angles and energies of both collisions, S_I and S_{II} , are chosen in such a way that $P_{12} = P_{23} = -1$, i.e. pure singlet scattering, we have

$$P^{(3)} = P^{(1)}, \quad (\text{A.32})$$

indicating a faithful quantum teleportation.

Fidelity

According to Popescu [32] the fidelity is defined as

$$F = \langle \psi_1 | \rho_3 | \psi_1 \rangle. \quad (\text{A.33})$$

Inserting BOB's density matrix (A.29) and the initial state amplitudes (A.2) yields

$$F = \frac{1}{2} (\alpha^*, \beta^*) \begin{pmatrix} 1 + P_{23} P_{12} p_z^{(1)} & P_{23} P_{12} (p_x^{(1)} - i p_y^{(1)}) \\ P_{23} P_{12} (p_x^{(1)} + i p_y^{(1)}) & 1 - P_{23} P_{12} p_z^{(1)} \end{pmatrix} \begin{pmatrix} \alpha \\ \beta \end{pmatrix}. \quad (\text{A.34})$$

Performing matrix multiplication with its bra and ket vectors, we obtain

$$F = \frac{1}{2} [|\alpha|^2 (1 + P_{12} P_{23} p_z^{(1)}) + \alpha^* \beta P_{12} P_{23} (p_x^{(1)} - i p_y^{(1)}) + \alpha \beta^* P_{12} P_{23} (p_x^{(1)} + i p_y^{(1)}) + |\beta|^2 (1 - P_{12} P_{23} p_z^{(1)})]. \quad (\text{A.35})$$

With the normalization condition (A.3) and using the parametrization (A.28) of the reduced density matrix in terms of the spin polarization vector, we can write

$$\begin{aligned} F &= \frac{1}{2} [1 + (|\alpha|^2 - |\beta|^2) P_{12} P_{23} p_z^{(1)} + P_{12} P_{23} p_x^{(1)} (\alpha^* \beta + \alpha \beta^*) \\ &\quad + P_{12} P_{23} p_y^{(1)} i (\alpha \beta^* - \alpha^* \beta)] \\ &= \frac{1}{2} [1 + P_{12} P_{23} (p_z^{(1)2} + p_x^{(1)2} + p_y^{(1)2})]. \end{aligned} \quad (\text{A.36})$$

Thus, we obtain the fidelity as a function of the two correlation parameters P_{12} and P_{23} , driving the first and second scattering processes, and the magnitude $|P^{(1)}|$ of the spin polarization vector of ALICE's electrons,

$$F = \frac{1}{2} (1 + P_{12} P_{23} |P^{(1)}|^2). \quad (\text{A.37})$$

In the case of a pure state to be teleported we have $|P^{(1)}| = 1$ and thus

$$F = \frac{1}{2} (1 + P_{12} P_{23}). \quad (\text{A.38})$$

For maximally entanglement in both scattering processes, that is $P_{12} = P_{23} = -1$, we get $F = 1$ which yields a faithful teleportation. In the case where ALICE's electrons are originally in a mixed state, we have $|P^{(1)}| < 1$ which always results in a reduction of fidelity. Even for maximal entanglement in both scattering processes we obtain

$$\frac{1}{2} \leq F = \frac{1}{2} (1 + |P^{(1)}|^2) < 1. \quad (\text{A.39})$$

References

- [1] Einstein A, Podolsky B and Rosen N 1935 Can quantum-mechanical description of physical reality be considered complete? *Phys. Rev.* **47** 777
- [2] Bennett C H, Brassard G, Popescu S, Crépeau C, Jozsa R, Peres A and Wootters W K 1993 teleporting an unknown quantum state via dual classical and Einstein-Podolsky-Rosen channels *Phys. Rev. Lett.* **70** 1895
- [3] Wootters W K and Zurek W H 1982 A single quantum cannot be cloned *Nature* **299** 802
- [4] Bouwmeester D, Pan J-W, Mattle K, Eible M, Weinfurter H and Zeilinger A 1997 Experimental quantum teleportation *Nature* **390** 575
- [5] Ma X-S *et al* 2012 Quantum teleportation over 143 kilometres using active feed-forward *Nature* **489** 269
- [6] Takeda S, Mizuta T, Fuwa M, van Loock P and Furusawa A 2013 Deterministic quantum teleportation of photonic quantum bits by a hybrid technique *Nature* **500** 315

- [7] Gottesman D and Chuang I L 1999 Demonstrating the viability of universal quantum computation using teleportation and single-qubit operations *Nature* **402** 390
- [8] Raussendorf R and Briegel H J 2001 A one-way quantum computer *Phys. Rev. Lett.* **86** 5188
- [9] Wang X-L, Cai X-D, Su Z-E, Chen M-C, Wu D, Li L, Liu N-L, Lu C-Y and Pan J-W 2015 Quantum teleportation of multiple degrees of freedom of a single photon *Nature* **518** 516
- [10] Ren J-G *et al* 2017 Ground-to-satellite quantum teleportation *Nature* **549** 70
- [11] Sherson J F, Krauter H, Olsson R K, Julsgaard B, Hammerer K, Cirac I and Polzik E S 2006 Quantum teleportation between light and matter *Nature* **443** 557
- [12] Reid M D, Drummond P D, Bowen W P, Cavalcanti E G, Lam P K, Bachor H A, Andersen U L and Leuchs G 2009 Colloquium: The Einstein-Podolsky-Rosen paradox: from concepts to applications *Rev. Mod. Phys.* **81** 1727
- [13] Marshall W, Simon C, Penrose R and Bouwmeester D 2003 Towards quantum superpositions of a mirror *Phys. Rev. Lett.* **91** 130401
- [14] Kwiat P G, Mattle K, Weinfurter H, Zeilinger A, Sergienko A V and Shih Y 1995 New high-intensity source of polarization-entangled photon pairs *Phys. Rev. Lett.* **75** 4337
- [15] Blum K and Lohmann B 2016 Entanglement and Bell correlation in electron-exchange collisions, *PRL* **116** 033201
- [16] Lohmann B, Blum K and Langer B 2016 Tunable entanglement resource in elastic electron-exchange collisions out of chaotic spin systems *Phys. Rev. A* **94** 032331
- [17] Hensen B *et al* 2015 Loophole-free Bell inequality violation using electron spins separated by 1.3 kilometres *Nature* **526** 682
- [18] Kelley M H, McClelland J J, Lorentz S R, Scholten R E and Celotta R J 1992 *Correlations and Polarization in Electronic and Atomic Collisions and (e, 2e) Reactions* ed P J O Teubner and E Weigold (Bristol: Institute of Physics) p 23
- [19] Baum G, Moede M, Raith W and Sillmen U 1986 Measurement of spin dependence in low-energy elastic scattering of electrons from lithium atoms *Phys. Rev. Lett.* **57** 1855
- [20] Bray I 1994 Convergent close-coupling calculation of electron-sodium scattering *Phys. Rev. A* **49** R1
- [21] Bray I, Fursa D V and McCarthy I E 1993 Calculation of electron-lithium scattering using the coupled-channel optical method *Phys. Rev. A* **47** 1101
- [22] Bartschat K and Fonseca dos Santos S 2017 Spin entanglement in elastic electron scattering from lithium atoms *Phys. Rev. A* **95** 042707
- [23] Kessler J 1985 *Polarized Electrons* 2nd edn (Berlin: Springer)
- [24] Clauser J F, Horne M A, Shimony A and Holt R A 1969 Proposed experiment to test local hidden-variable theories *Phys. Rev. Lett.* **23** 880
- [25] Taylor J R 1972 *Scattering Theory* (New York: Wiley)
- [26] Dieks D 1982 Communication by EPR devices *Phys. Lett.* **92A** 271
- [27] Zukowski M, Zeilinger A, Horne M A and Ekert A 1993 'Event-Ready-Detectors' Bell experiment via entanglement swapping *Phys. Rev. Lett.* **71** 4287
- [28] Bose S, Vedral V and Knight P L 1998 Multiparticle generalization of entanglement swapping *Phys. Rev. A* **57** 822
- [29] Klyachko A A 2006 Quantum marginal problem and N-representability *J. Phys.: Conf. Ser.* **36** 72
- [30] Altunbulak M and Klyachko A A 2008 The Pauli principle revisited *Commun. Math. Phys.* **282** 287
- [31] Schilling C, Benavides-Riveros C L and Vrana P 2017 Reconstructing quantum states from single-party information *Phys. Rev. A* **96** 052312
- [32] Popescu S 1994 Bell's inequalities versus Teleportation: what is nonlocality? *Phys. Rev. Lett.* **72** 797
- [33] Horodecki R, Horodecki M and Horodecki P 1996 Teleportation, Bell's inequalities and inseparability *Phys. Lett. A* **222** 21
- [34] Burke P G and Schey H 1962 Polarization and correlation of electron spin in low-energy elastic electron-hydrogen collisions *Phys. Rev.* **126** 163
- [35] Kleinpoppen H, Lohmann B and Grum-Grzhimailo A N 2013 *Perfect/Complete Scattering Experiments—Probing Quantum Mechanics on Atomic and Molecular Collisions and Coincidences* (Berlin: Springer)
- [36] Blum K 2012 *Density Matrix Theory and Applications* 3rd edn (Berlin: Springer) in particular section 3.6.5.